We have now found that photooxidation of diphenyldiazomethane in an aldehyde solvent leads to the formation of the appropriate ozonide, incorporating the aldehyde and zwitterion, **2**, and the suppression of diperoxide formation. This ozonide formation represents a duplication of the Criegee ozonolysis mechanism[5] under conditions where no ozone is involved.

It seems likely that the intermediate involved in the ozonide formation has the zwitterion form, **2**, inasmuch as the carbonyl oxides produced in ozonolysis, and presumably duplicated here, do not show radical character.[5] On the other hand, the low yields of ozonide and the earlier results of Hamilton and Giacin[4] suggest that the diradical species, **1**, is produced initially. This intermediate could then be converted to **2** for the ozonide reaction or undergo further radical reactions.

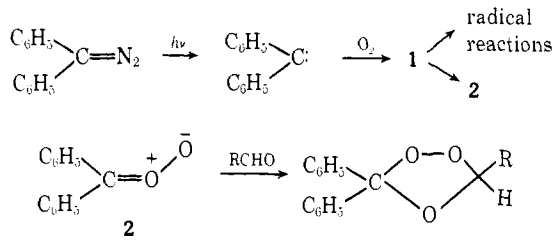

When a solution of 18.9 g of diphenyldiazomethane in 125 ml of chlorobenzene was photooxidized[6] using an oxygen flow of 240 ml/min the diazo compound was completely decomposed in 2 hr. After removal of the solvent the yellow residue was recrystallized from acetone to give 1.26 g of solid benzophenone diperoxide, mp 210–212° (lit.[2] mp 213.5–214°). A solution of 9.70 g of diphenyldiazomethane in 200 ml of freshly distilled acetaldehyde was photooxidized for 130 min with an oxygen flow rate of 300 ml/min. After removal of excess acetaldehyde under reduced pressure the yellow residue was chromatographed on silica gel. Elution with hexane–benzene (80:20) gave 0.95 g (7.8%) of 1,1-diphenylpropene ozonide. This material was identical with that obtained from ozonolysis of 1,1-diphenylpropene and had nmr absorptions[8] at 2.7 (multiplet, 10 H), 4.50 (quartet, 1 H), and 8.60 (doublet, 3 H), and infrared absorptions at 1220 and 1120 cm^{-1}. Further elution of the column with benzene–hexane (50:50) gave 8.23 g (90.5%) of benzophenone. The absence of benzophenone diperoxide in the photooxidation in the presence of acetaldehyde is presumably due to the successful competition of the aldehyde for the zwitterions at the expense of the dimerization process.

Similar photooxidations using propionaldehyde and benzaldehyde as solvents led to the formation of 1,1-diphenyl-1-butene (0.8%) and triphenylethylene (11.8%) ozonides, respectively. The 1,1-diphenyl-1-butene ozonide had nmr absorptions at 2.7 (multiplet, 10 H), 4.57 (triplet, 1 H), 8.0–8.9 (multiplet, 2 H), and 9.02 (triplet, 3 H). The triphenylethylene ozonide had nmr absorptions at 2.7 (multiplet, 15 H) and 3.73 (singlet, 1 H) and mp 97° (lit.[9] mp 95°).

These observations lend additional support to the mechanism proposed[1] for the photooxidation of diphenyldiazomethane. At the same time they can provide a unique confirmation of the proposal of Criegee[5] that ozonides arise from the addition of carbonyl oxides to carbonyl compounds. This process also provides a synthetic route to ozonides which does not involve ozonolysis. Because of our interest in the mechanism of ozonolysis[10] we intend to conduct similar photooxidations of diazo compounds under conditions where ozonide cis–trans pairs can be expected. The stereochemical results so obtained could then be compared to those obtained from the ozonolysis of the suitable olefin.

Acknowledgment. This work was supported by the National Science Foundation through Grants GP 10895 and GP 29373X.

(5) R. Criegee, *Rec. Chem. Progr.*, **18**, 111 (1957).

(6) The photooxidation apparatus used was similar to that described in the literature.[7] A General Electric DWY 650-W lamp was used without filter.

(7) C. S. Foote, S. Wexler, W. Ando, and R. Higgins, *J. Amer. Chem. Soc.*, **90**, 975 (1968).

(8) Nmr values given are τ values relative to internal TMS and were taken in CCl_4.

(9) J. Castonguay, M. Bertrand, J. Carles, S. Fliszár, and Y. Rousseau, *Can. J. Chem.*, **47**, 919 (1969).

(10) See, for example, R. W. Murray, *Accounts Chem. Res.*, **1**, 313 (1968).

R. W. Murray,* A. Suzui
Department of Chemistry, University of Missouri-St. Louis
St. Louis, Missouri 63121
Received June 11, 1971

Lattice Spacings of Pseudobinary Solid Solutions of Silver Bromide and Silver Iodide

Sir:

Laboratory and cloud-seeding experiments in the natural atmosphere have established that silver iodide particles are effective in nucleating the formation of ice crystals in supercooled water and in regions supersaturated with respect to ice. It is recognized that the close similarity of the crystal structure of silver iodide to that of ice may be one of the factors that make it a good nucleus.[1]

In the close packing of the cubic system the atomic layers are stacked along the body diagonal in an ABCABC... arrangement, while in the case of close packing in the hexagonal system the atoms are stacked along the hexagonal direction in the ABAB... sequence. Both structures have the same atomic arrangement in the planes; that is, each atom has 12 equidistant nearest neighbors, 6 in its own plane and 3 in each adjacent layer. The next-nearest neighbors are arranged differently in the two cases. Each structure can be made equivalent to the other by a rotation of half the crystal of 30° about the crystallographic directions defined above. Thus, at the ice–AgI interface, lattice coherence can be achieved between the two crystal structures but two effects now prevail. There is a misfit strain between the ice–AgI interface due to a small difference in the lattice spacings between these two structures, and a stacking fault is introduced at the interface. The implications of the dislocations at the interface have been discussed by Turnbull and Vonnegut.[2] In the same publication, Turnbull and

(1) B. Vonnegut, *J. Appl. Phys.*, **19**, 959 (1948); *Bull. Amer. Meteorol. Soc.*, **31**, 151 (1950); B. Vonnegut and K. Maynard, *ibid.*, **33**, 420 (1952); B. Vonnegut, *ibid.*, **50**, 248 (1969).

Table I. Lattice Parameters of the Pseudobinary Solid Solutions of AgBr and AgI

	AgI solid solutions			AgBr solid solutions		
Mol % AgBr	Lattice parameters, Å	Closest approach,[a] Å	Disregistry, δ[b]	Lattice parameters, Å	Closest approach,[a] Å	Disregistry, δ[b]
0	$a = 4.5834$					
0	$c = 7.5243$	4.5834	1.55			
5	$a = 6.4779$	4.5806	1.49			
10	$a = 6.4780$	4.5807	1.49			
15	$a = 6.4665$	4.5726	1.31			
20	$a = 6.4598$	4.5678	1.20			
25	$a = 6.4566$	4.5655	1.15			
30	$a = 6.4455$	4.5577	0.98			
50	$a = 6.4445$	4.5569	0.96			
30				$a = 5.8845$	4.1609	−7.81
50				$a = 5.8823$	4.1594	−7.83
60				$a = 5.8830$	4.1599	−7.84
85				$a = 5.8332$	4.1247	−8.61
100				$a = 5.7750$	4.0835	−9.53
Ice	$a = 4.5135$					
Ice	$c = 7.3521$	4.5135				

[a] Closest approach = average distance of closest approach of the atoms. [b] Disregistry = [distance of closest approach − a(ice)]/a(ice) × 100.

Vonnegut suggest that the interfacial strain between the (001) plane of ice and a low-index plane of the artificial nucleating agent can be placed on a quantitative basis by defining a disregistry, $\delta = |\Delta a/a_0|$. These workers note that experimental observations lead to the indications that the order of potency of catalysts corresponds to the order of the reciprocal of the disregistries ($1/\delta$) on low-index planes. In view of this postulate and the fact that the pertinent lattice parameters for AgI and ice are $a_0 = 4.5834$ and 4.5135 Å, respectively, it was felt that it would be interesting to study the effect of decreasing the disregistry δ by decreasing the lattice parameter of AgI. This study was undertaken to determine the relationship between lattice constants and nucleation of AgI.

A convenient method for varying the lattice parameter of AgI in a continuous way is to form a series of terminal solid solutions.[3] In the case at hand, the suitable unit cell volumes of AgI and ice are 136.13 and 129.71 Å^3 at room temperature and 0°, respectively. The pseudobinary solid solutions of AgBr and AgI were considered promising for this purpose, since the bromine atom is considerably smaller than the iodine atom and would, therefore, reduce the lattice spacing of the AgI lattice. The AgBr–AgI system forms two terminal solid solutions at room temperature,[4] one at the AgI-rich side of the phase diagram and the other at the AgBr-rich side. Thus, one could hope to approach agreement with the unit cell volume of ice from either end of the constitution diagram.

Samples of crystalline silver halides were prepared by precipitation from aqueous solutions. Stock solutions were prepared by mixing 0.78 *N* NaI and 0.78 *N* NaBr solutions in various proportions ranging in 5% steps from 100% NaI to 100% NaBr. The silver halide was precipitated by pouring together in a test tube 5 ml of the sodium halide solution with a slight excess (about 5.5 ml) of 0.78 *N* $AgNO_3$ solution. After the two solutions had been added together and thoroughly mixed by shaking, the resultant precipitate was rinsed repeatedly by allowing it to settle and washed with deionized water by decantation. Examination by optical and electron microscopy revealed that the precipitate consisted of clumps of the order of 50-μ diameter composed of agglomerated small crystals of the order of 1 μ or less in size. Figure 1 shows an electron micrograph of the 20% AgI, 80% AgBr precipitate deflocculated with an ultrasonic generator.

The isolated precipitated powders were washed in distilled water, dried in air, and passed through a 400-mesh sieve. The sifted powders were then placed in a 0.5-mm diameter quartz capillary and sealed off. X-Ray diffraction diagrams were taken before and after annealing at 100° for 8 hr, but no sensible changes in the X-ray diagrams were detected. Powder diagrams were taken in a 114.59-mm diameter Debye–Scherrer camera for 24 hr, employing a cobalt-target X-ray tube and an iron-foil filter to minimize the appearance of the Kβ lines on the diagram. The wavelengths used were $\lambda_{K\alpha} = 1.79021$, $\lambda_{K\alpha_1} = 1.78892$, and $\lambda_{K\alpha_2} = 1.79278$ Å. No lines were observed that could not be indexed on the basis of one of the phases shown in the constitution diagram. A small amount of high-purity silicon powder was mixed with the samples before sealing off, and their diffraction lines served as fiducial marks to determine film shrinkage due to processing. It is estimated from these measurements that a precision of 1 part in 10,000 was obtained in this work. Broadening of the diffraction lines was observed in the back-reflection region of the diagrams which did not change appreciably on annealing. This implies that the line broadening was due to particle size or that annealing was not carried out to completion. Corrections for camera radius error, absorption of X-rays by the sample, and sample eccentricity with respect to the primary beam were made by plotting the calculated lattice spacings against the Nelson–Riley function.

The results of the lattice parameter measurements are given in Table I, and the data are plotted in Figure 2. Closest approach refers to the average distance of closest approach of the atoms in the lattice and is represented by $a\sqrt{2}/2$ for the cubic system, while it is

(2) D. Turnbull and B. Vonnegut, *Ind. Eng. Chem.*, **44**, 1292 (1952).
(3) W. B. Pearson, "A Handbook of Lattice Spacings and Structures of Metals and Alloys," Pergamon Press, New York, N. Y., 1958; H. W. King in "Effects in Concentrated Solid Solutions," T. B. Massalski, Ed., Gordon and Breach, New York, N. Y., 1965; H. Chessin, S. Arajs and D. S. Miller, *Advan. X-Ray Anal.*, **6**, 121 (1963).
(4) O. Stasiw and J. Teltow, *Z. Anorg. Chem.*, **259**, 143 (1949).

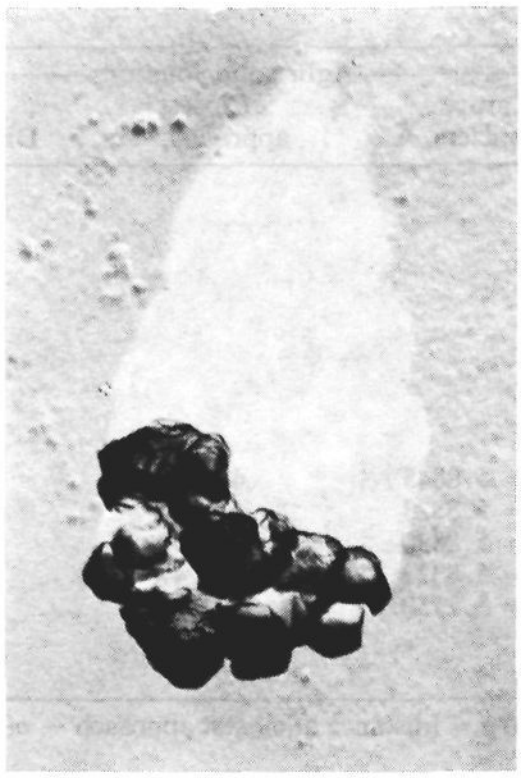

Figure 1. Electron micrograph of coprecipitated particles of 20 mol % AgI, 80 mol % AgBr. The particles were deflocculated ultrasonically. Magnification: 50,000×.

the lattice spacing in the basal plane in the hexagonal system. The disregistry expresses the difference between the atomic spacings in the close-packed plane (the 111 plane) in the cubic system and the basal plane of the ice lattice. The significance of this quantity was discussed above. In the tables, the terms AgI solid solutions and AgBr solid solutions refer to the terminal solid solutions formed with AgI and AgBr as the solvents, respectively. In Figure 2 the distances of closest approach ($a\sqrt{2}/2$) are plotted and compared to that of ice. Thus the difference between the two curves represents the packing difference in the closest packed planes, or the disregistry, between the solid solutions and the ice lattice. The component phases that are present in the X-ray powder diagrams are listed in Table II.

Table II. Compositions of AgBr–AgI Solid Solutions

Mol % AgBr	Phases present
5	AgI solid solution
10	AgI solid solution
15	AgI solid solution
	AgBr solid solution
30	AgI solid solution
	AgBr solid solution
60	AgI solid solution
	AgBr solid solution
	AgBr
85	AgBr solid solution

It is well known[5] that the leveling off of the lattice parameters in solid solutions indicates the limit of solubility of the solute in the solvent. It is clear from Figure 2 that the limit of solubility of AgBr in AgI in this experiment is approximately 28 mol % and the solubility of AgI in AgBr is approximately 30 mol %. According to the constitution diagram of Stasiw and Teltow,[4] the solubility of AgI in AgBr is about 16

(5) C. S. Barrett and T. B. Massalski, "Structure of Metals," McGraw-Hill, New York, N. Y., 1966.

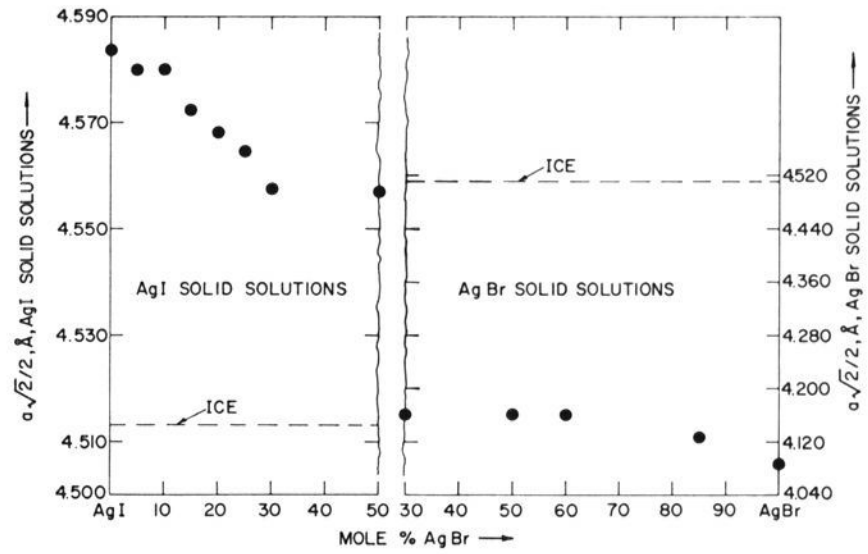

Figure 2. Average distance of closest approach in close-packed planes of AgI–AgBr solid solutions.

mol %, while up to 50 mol % AgBr can be substituted in the AgI lattice at 127°. However, the conditions of our experiment are such that in all likelihood thermodynamic equilibrium was not reached, accounting for the high solubility of AgI in AgBr. Further studies will be reported shortly elsewhere on our observations of the ice-nucleating efficiency of these solid solutions.

Acknowledgments. This work was sponsored in part by the Office of Naval Research under Contract No. N00014-71-C-0156 and in part by the Air Force Cambridge Research Laboratories, Office of Aerospace Research, under Contract No. F19628-68-C-0057. This report does not necessarily reflect endorsement by the sponsors.

(6) (a) Department of Physics; (b) Department of Atmospheric Science and Senior Research Scientist, Atmospheric Sciences Research Center.

Henry Chessin,*[6a] Bernard Vonnegut[6b]
State University of New York at Albany
Albany, New York 12203
Received July 15, 1971

The Geometry of [10]Annulenes

Sir:

Since Hückel's prediction of aromaticity for certain monocyclic polyenes in 1931,[1] chemists' interest in [10]annulenes has been evident and attempts at the synthesis of this system date back presumably to the early part of this century when Willstätter accomplished the first synthesis of cyclooctatetraene.[2] We wish to record herein that we have now prepared two *crystalline* (below −60°) [10]annulenes, **1** and **2**, and to present evidence to establish the double bond geometry of these molecules. Temperature-dependent ^{13}C nmr spectroscopy has been employed to elucidate a unique automerization[3] of compound **2**. This instance represents one of the first—if not the first—example of its application to this type of problem.

After a critical evaluation of possible synthetic routes leading to **1** and/or **2** we reached the conclusion that one similar to that reported earlier[4] is a *practical*

(1) E. Hückel, *Z. Phys.*, **70**, 204 (1931).
(2) R. Willstätter and E. Wase, *Ber.*, **44**, 3423 (1911).
(3) A. T. Balaban and D. Farcasiu, *J. Amer. Chem. Soc.*, **89**, 1958 (1967).